
FORECASTING SYMMETRIC RANDOM WALKS: A FUSION APPROACH

Cheng Zhang[†]
Hubei Polytechnic University
Huangshi, China
zcheng582dx@gmail.com

ABSTRACT

Forecasting random walks is notoriously challenging, with naïve prediction serving as a difficult-to-surpass baseline. To investigate the potential of using movement predictions to improve point forecasts in this context, this study focuses on symmetric random walks, in which the target variable's future value is reformulated as a combination of its future movement and current value. The proposed forecasting method, termed the fusion of movement and naïve predictions (FMNP), is grounded in this reformulation. The simulation results show that FMNP achieves statistically significant improvements over naïve prediction, even when the movement prediction accuracy is only slightly above 0.50. In practice, movement predictions can be derived from the comovement between an exogenous variable and the target variable and then linearly combined with the naïve prediction to generate the final forecast. FMNP effectiveness was evaluated on four U.S. financial time series—the close prices of Boeing (BA), Brent crude oil (OIL), Halliburton (HAL), and Schlumberger (SLB)—using the open price of the Financial Times Stock Exchange (FTSE) index as the exogenous variable. In all the cases, FMNP outperformed the naïve prediction, demonstrating its efficacy in forecasting symmetric random walks and its potential applicability to other forecasting tasks.

Keywords Symmetric random walk · Fusion · Movement prediction · Naïve prediction · Point forecasting

1 Introduction

A random walk is a stochastic process where each data point is generated by adding a random increment, typically drawn from a specified probability distribution, to the previous data point. It is characterized by a memoryless property and stepwise random changes (Pearson, 1905). A diverse array of real-world time series can be modeled as random walks, including financial time series, such as stock prices, and physical phenomena, such as fluctuations in physical systems. The dependence between one time step and the next in a random walk provides a certain degree of consistency, thereby avoiding the large jumps that are characteristic of a purely random series (Wergen et al., 2012). Consequently, strong autocorrelation can be observed between two adjacent data points, and the random walk series is often nonstationary, with the variance changing over time.

A further defining feature of a random walk is that its future values are deemed unpredictable. Any attempt to predict a random walk is tantamount to predicting a series of random events (Fama, 1995; Y.-C. Zhang, 1999). Stock market data provide an illustrative example of a random walk, characterized by a vast amount of data, yet stock prices are often considered almost unpredictable (Engle, 2004). Moosa (2013) demonstrated through simulation that as the volatility of a financial time series increases, the root mean square error (RMSE) of forecasting models increases faster than that of the naïve prediction, which is a simple but robust forecasting benchmark that predicts the future value to be the same as the current observed value. Furthermore, Moosa and Burns (2014) argue that claims of beating the naïve prediction in terms of the RMSE are often misleading, as they frequently involve introducing dynamics without proper statistical

[†]: <https://orcid.org/0000-0002-4150-3371>

testing. Naïve prediction is a strong and reliable baseline in random walk forecasting, often posing a challenge for complex methods to surpass it (Kilian & Taylor, 2003; Moosa & Burns, 2016).

Despite the skepticism of the efficacy of point forecasting in random walks, this task remains indispensable because of the high demand for point forecasting in various fields, such as financial time series forecasting, which has led to the development of numerous forecasting methods. For example, statistical methods, such as autoregressive integrated moving average (ARIMA), and machine learning techniques, such as artificial neural networks (ANNs) and support vector regression (SVR), have been developed to model and predict financial time series (Adhikari & Agrawal, 2014; Cheng et al., 2015; Jiang, 2021). In recent years, deep learning techniques have significantly advanced forecasting models. Recurrent neural networks (RNNs), particularly long short-term memory (LSTM) networks, have proven highly effective in capturing temporal dependencies in sequential data and have been widely applied to financial market predictions (Lara-Benítez et al., 2021; Sezer et al., 2020). Additionally, convolutional recurrent neural networks (CRNNs), which combine the ability of convolutional neural networks (CNNs) to identify spatial patterns with the strength of RNNs in analyzing temporal data, have been applied to the forecasting of financial time series (Tsantekidis et al., 2020). Moreover, transformer-based models such as Autoformer and FEDformer, which were initially designed for natural language processing, have also been tested in financial time series forecasting, highlighting their versatility in handling sequential data and capturing long-range dependencies (H. Wu et al., 2021; Zhou et al., 2022).

Unfortunately, the effectiveness of these statistical, machine learning, and deep learning methods typically falls short of that of naïve predictions (Ellwanger & Snudden, 2023; Hewamalage et al., 2023; Petropoulos et al., 2022; Thakkar & Chaudhari, 2021; Zeng et al., 2023). Although financial time series are widely used for testing neural networks, their results often lack generalizability due to their sensitivity to hyperparameters and data snooping bias, where extensive tuning produces good results on specific datasets that cannot be extended to others (Petropoulos et al., 2022). Notably, different types of forecasting methods based on time–frequency decomposition have been shown to outperform naïve baselines in random walk forecasting (Hewamalage et al., 2023; C. Zhang et al., 2024). However, these methods often include future information in the training data, leading to measured accuracy under data leakage scenarios (Hewamalage et al., 2023; C. Wu et al., 2022; J.-L. Zhang et al., 2015). When data leakage is explicitly avoided during data preprocessing, the accuracy of the prediction often falls below that of naïve prediction (Hewamalage et al., 2023). In general, whether these complicated methods in random walk forecasting are effective remains a subject of debate and an open question.

In addition to advanced forecasting models with complex structures, feature-based forecasting has emerged as a prominent data-driven approach. This method improves point forecasts by leveraging a diverse set of features derived from both internal and external data sources (Petropoulos et al., 2022). One notable study by Baumeister et al. (2015) successfully employed high-frequency stock indices to forecast crude oil monthly prices via a mixed data sampling (MIDAS) model, reducing the mean square prediction error (MSPE) by as much as 28% compared with the naïve baseline and achieving a directional accuracy of 73%. While this study demonstrated that point forecasts for certain financial time series are possible under the right conditions, most research has shifted from point forecasting to movement prediction because the latter can easily outperform the random guess if the performance of the prediction is judged according to criteria such as movement prediction accuracy (Moosa, 2013; Taylor, 2008). For example, Weng et al. (2017) incorporated Google news count and Wikipedia page views alongside historical data to predict the next day's movement of AAPL stock via support vector machines (SVMs) and decision trees, achieving up to 80% movement prediction accuracy. Ma et al. (2023) proposed a multisource aggregated classification (MAC) method for stock price movement prediction, incorporating the numerical features and market-driven news sentiments of target stocks, as well as the news sentiments of their related stocks, and the movement prediction accuracy can reach as high as 70%. Depending on the complexity of the markets and the availability of data, movement prediction accuracy in financial time series typically ranges between 0.55 and 0.80 (Bustos & Pomares-Quimbaya, 2020). However, the valuable directional information yielded by these movement prediction methods has yet to be leveraged to increase the accuracy of point forecasts.

Moreover, a widely accepted practice in the field of forecasting is that exogenous variables within a forecasting system are not being predicted; instead, the current value of an exogenous variable is frequently employed as a feature to predict the future value of the target variable (Petropoulos et al., 2022). This approach is based on the assumption that the current value of an exogenous variable may provide additional predictive power if it is highly correlated with the future value of the target variable. However, in the case of random walk forecasting, even if there is a high correlation between two such sequences of values, the current value of the exogenous variable may still have no more predictive power beyond the current value of the target variable, as the latter tends to be highly correlated with its own future value as well. Importantly, in addition to the information conveyed by the current value of the target variable, comovement between exogenous variables and the target variable can provide additional predictive information (Christen et al., 2022; Scabbia et al., 2020). Therefore, it is reasonable to use the comovement between exogenous variables and the target variable to improve predictions and to use the future movement or predicted movement of the exogenous variable (rather

than its current value) as a predictor because comovement tends to be strongest when the two variables are synchronized. This also means that if the movement of the target variable is accurately predicted, it can be used as a predictor for point forecasting because the comovement between accurate movement prediction and actual future movement is also strong.

Therefore, in the context of random walk forecasting, utilizing movement predictions—either from the target variable itself or from exogenous variables with strong comovement—has the potential to improve point forecasting results beyond the naïve baseline. Considering the significant focus on point forecasting in random walks, this potential is worth investigating. This study aims to explore, in random walk forecasting, how movement predictions can be incorporated into point forecasting and whether such a forecasting approach is effective. In particular, symmetric random walks are used as the pivotal forecasting target, as they are characterized by the absence of drift and equal probabilities of upward and downward movements (Ibe, 2014) and are well suited for investigating the effectiveness of utilizing movement prediction for point forecasting in random walks. To this end, the process of symmetric random walks is reformulated to explicitly incorporate future movements, and on the basis of this reformulation, a method for point forecasting in symmetric random walks, referred to as fusion of movement and naïve predictions (FMNP), is proposed. Given the inherent difficulty of predicting the movement of the target variable directly, movement predictions can be derived from the comovement between an exogenous variable and the target variable. Specifically, the movement prediction of an exogenous variable that consistently exhibits strong comovement with the target variable can be used as the movement prediction for the target variable. This movement prediction and the naïve prediction are combined linearly to generate the final point forecast.

The effectiveness of the FMNP method was evaluated through simulations using synthetic data and real-world experiments on four financial time series from U.S. markets. The real-world data included the close prices of Boeing Company (BA), Halliburton Company (HAL), Schlumberger Limited (SLB), and Brent crude oil (OIL), with the open price of the Financial Times Stock Exchange (FTSE) index serving as the exogenous variable. For all the experiments, the naïve prediction serves as the sole baseline, with the RMSE, mean absolute error (MAE), mean absolute percentage error (MAPE) and symmetric mean absolute percentage error (sMAPE) used as evaluation metrics.

This study makes three significant contributions to the literature:

- The FMNP method, which is based on the reformulation of symmetric random walks, bridges movement prediction and point prediction—two distinct tasks in random walk forecasting. While the use of binary classification to guide regression is well established, leveraging the target variable’s movement prediction to inform its point forecast introduces a novel perspective. The FMNP method can be regarded as a type of classification-to-regression conversion that transforms binary data into continuous data and facilitates the integration of diverse data types for enhanced decision-making.
- This study introduces a novel optimization strategy that simplifies the optimization of the proposed FMNP method in the context of random walk forecasting. Unlike traditional approaches that find the optimal parameter by minimizing the loss function, such as the mean squared error (MSE), this strategy focuses on maximizing the MSE difference between the naïve and fusion predictions, avoiding the issue that the stochastic error term cannot be analytically eliminated when calculating the derivative of the loss function.
- The FMNP method has the ability to surpass naïve prediction in multiple financial time series forecasting tasks by incorporating patterns beyond historical prices, such as comovement between exogenous and target variables. This observation suggests that opportunities for limited predictability do exist in financial time series forecasting, prompting further exploration of the assumption underlying the strong form of the efficient market hypothesis (EMH) (Fama, 1995).

In summary, this study introduces a new approach to point forecasting in symmetric random walks, providing a strong theoretical foundation for the method and demonstrating its effectiveness through real-world applications. Based on current knowledge, the FMNP method is the first to robustly outperform naïve prediction while presenting strong generalization capabilities in the context of random walk forecasting.

The remainder of this paper is organized as follows. Section 2 introduces the details of the proposed FMNP method. Section 3 presents a simulation study that assesses the proposed FMNP method via synthetic datasets under controlled experiments. Section 4 demonstrates the performance of the FMNP method on real-world datasets, presenting details of the results and analysis. Finally, the discussion section covers key findings, limitations, and implications, while the last section concludes this study and outlines future directions.

2 FMNP

This section first introduces a reformulation of symmetric random walks, which serves as the theoretical basis for the proposed FMNP method. Furthermore, the optimization of FMNP is achieved by maximizing the MSE difference

between the naïve and fusion predictions, thereby identifying the conditions under which the fusion prediction outperforms the naïve prediction by the maximum margin.

2.1 Theoretical Basis of FMNP

A symmetric random walk is a stochastic process where the value at time step t depends on the value at the previous time step $t - 1$ and an independent random increment ϵ_t , which is typically assumed to follow a normal distribution with mean 0 and variance σ_t^2 (De Gooijer et al., 2017). The general formulation is as follows:

$$y_t = y_{t-1} + \epsilon_t, \epsilon_t \sim \mathcal{N}(0, \sigma_t^2), \quad (1)$$

where y_t is the point value at time step t and y_{t-1} is the point value at time step $t - 1$. For random walks with homoscedasticity, σ_t^2 is constant over time, and for random walks with heteroscedasticity, σ_t^2 changes over time. The symmetric nature of the probability distribution of the random increment ϵ_t with a mean of 0 ensures no inherent bias in the movement direction of the target variable and that upward and downward movements are equally likely (Ibe, 2014). To incorporate the future movement direction of the target variable into the general formulation, ϵ_t can be expressed as a product of two components: a positive random increment ϵ_t^+ representing the magnitude of the increment and a sign component D_t , which takes the value +1 for upward movement and -1 for downward movement, indicating the direction of the increment between two adjacent points. For a symmetric random walk, this allows the process to be reformulated as follows:

$$y_t = y_{t-1} + D_t \cdot \epsilon_t^+; \epsilon_t^+ > 0 \quad (2)$$

Since the positive increments ϵ_t^+ are also independent, they are theoretically unpredictable. Nonetheless, ϵ_t^+ can further be expressed as a product of two positive terms:

$$y_t = y_{t-1} + D_t \cdot \theta_t \cdot \bar{\epsilon}; \theta_t > 0, \bar{\epsilon} > 0, \quad (3)$$

where $\bar{\epsilon}$ represents the mean absolute increment calculated from previous time steps, which can be interpreted as a base magnitude of the increments. The term θ_t is introduced as a positive weight that controls the magnitude of the increment at time step t . Eq. (3) implies that the point forecast of the target variable can be derived if D_t and θ_t are provided. Consider a simple scenario in which the magnitude of the increment between two adjacent points is fixed for out-of-sample prediction; then, θ_t can be set to a constant value in advance. Consequently, the point forecast for future time step t , denoted as \hat{y}_t , can be expressed as follows:

$$\hat{y}_t = y_{t-1} + \hat{D}_t \cdot \theta \cdot \bar{\epsilon}; \theta > 0, \bar{\epsilon} > 0, \quad (4)$$

where \hat{D}_t is the movement prediction, θ is a fixed scalar, and $\theta \in \mathbb{Q}^+$. Eq. (4) serves as the foundation of the proposed forecasting method, FMNP, in which the naïve prediction y_{t-1} and movement predictions \hat{D}_t are the method's inputs and θ and $\bar{\epsilon}$ are parameters.

2.2 Optimization of FMNP

Suppose that the movement prediction \hat{D}_t is provided and that the mean absolute increment $\bar{\epsilon}$ has been determined on the basis of the training set; then, the performance of FMNP depends only on the setting of θ . However, the tuning of θ on the basis of the training set by minimizing the loss function, typically the MSE, is challenging because the stochastic component ϵ_t^+ cannot be analytically eliminated when calculating the derivative of the loss function with respect to θ . Nonetheless, it should be recognized that the MSE of the naïve prediction is a fixed value given a training set. Therefore, minimizing the MSE of the fusion prediction is equivalent to maximizing the MSE difference between the naïve and fusion predictions:

$$\min MSE_{\text{train}}^{\text{FMNP}} \equiv \max (MSE_{\text{train}}^{\text{naïve}} - MSE_{\text{train}}^{\text{FMNP}}) \quad (5)$$

Suppose the movement prediction consists of $n_{\text{train}}^{\text{correct}}$ directions that are correct and $n_{\text{train}}^{\text{incorrect}}$ directions that are incorrect across the training set with N time steps; then, the MSEs of the naïve and fusion predictions on the training set can be further expressed as follows:

$$\begin{aligned} MSE_{\text{train}}^{\text{naïve}} &= \frac{1}{N} \left(\sum_{t \in \text{train}} (y_t - y_{t-1})^2 \right) \\ &= \frac{1}{N} \left(\sum_{t \in \text{train}} (y_{t-1} + D_t \cdot \epsilon_t^+ - y_{t-1})^2 \right) \\ &= \frac{1}{N} \left(\sum_{t \in \text{correct}} (\epsilon_t^+)^2 + \sum_{t \in \text{incorrect}} (\epsilon_t^+)^2 \right) \end{aligned} \quad (6)$$

$$\begin{aligned}
 MSE_{\text{train}}^{\text{FMNP}} &= \frac{1}{N} \left(\sum_{t \in \text{train}} (y_t - \hat{y}_t)^2 \right) \\
 &= \frac{1}{N} \left(\sum_{t \in \text{correct}} (y_t - \hat{y}_t)^2 + \sum_{t \in \text{incorrect}} (y_t - \hat{y}_t)^2 \right) \\
 &= \frac{1}{N} \left(\sum_{t \in \text{correct}} \left[(y_{t-1} + D_t \cdot \epsilon_t^+) - (y_{t-1} + \hat{D}_t \cdot \theta_{\text{train}} \cdot \bar{\epsilon}_{\text{train}}) \right]^2 \right. \\
 &\quad \left. + \sum_{t \in \text{incorrect}} \left[(y_{t-1} + D_t \cdot \epsilon_t^+) - (y_{t-1} + \hat{D}_t \cdot \theta_{\text{train}} \cdot \bar{\epsilon}_{\text{train}}) \right]^2 \right) \\
 &= \frac{1}{N} \left(\sum_{t \in \text{correct}} \left((\epsilon_t^+)^2 - 2\theta_{\text{train}} \cdot \epsilon_t^+ \cdot \bar{\epsilon}_{\text{train}} + \theta_{\text{train}}^2 \cdot \bar{\epsilon}_{\text{train}}^2 \right) \right. \\
 &\quad \left. + \sum_{t \in \text{incorrect}} \left((\epsilon_t^+)^2 + 2\theta_{\text{train}} \cdot \epsilon_t^+ \cdot \bar{\epsilon}_{\text{train}} + \theta_{\text{train}}^2 \cdot \bar{\epsilon}_{\text{train}}^2 \right) \right), \tag{7}
 \end{aligned}$$

where θ_{train} represents the fixed weight for the training set and $\bar{\epsilon}_{\text{train}}$ denotes the mean of ϵ_t^+ calculated over the training set. On the basis of the law of large numbers (LLN) and that ϵ_t^+ is a positive random term, when both $n_{\text{train}}^{\text{correct}}$ and $n_{\text{train}}^{\text{incorrect}}$ are sufficiently large, $\sum_{t \in \text{correct}} \epsilon_t^+$ approximates $n_{\text{train}}^{\text{correct}} \cdot \bar{\epsilon}_{\text{train}}$ and $\sum_{t \in \text{incorrect}} \epsilon_t^+$ approximates $n_{\text{train}}^{\text{incorrect}} \cdot \bar{\epsilon}_{\text{train}}$. According to Eqs. (5), (6), and (7), the MSE difference between the naïve and fusion predictions on the training set can be further expressed as follows:

$$\begin{aligned}
 \Delta MSE_{\text{train}} &= MSE_{\text{train}}^{\text{naïve}} - MSE_{\text{train}}^{\text{FMNP}} \\
 &= \frac{1}{N} \left(\sum_{t \in \text{correct}} (\epsilon_t^+)^2 + \sum_{t \in \text{incorrect}} (\epsilon_t^+)^2 \right) - \frac{1}{N} \left(\sum_{t \in \text{correct}} \left((\epsilon_t^+)^2 - 2\theta_{\text{train}} \cdot \epsilon_t^+ \cdot \bar{\epsilon}_{\text{train}} + \theta_{\text{train}}^2 \cdot \bar{\epsilon}_{\text{train}}^2 \right) \right. \\
 &\quad \left. + \sum_{t \in \text{incorrect}} \left((\epsilon_t^+)^2 + 2\theta_{\text{train}} \cdot \epsilon_t^+ \cdot \bar{\epsilon}_{\text{train}} + \theta_{\text{train}}^2 \cdot \bar{\epsilon}_{\text{train}}^2 \right) \right) \\
 &= \frac{1}{N} \left(\sum_{t \in \text{correct}} \left(2\theta_{\text{train}} \cdot \epsilon_t^+ \cdot \bar{\epsilon}_{\text{train}} - \theta_{\text{train}}^2 \cdot \bar{\epsilon}_{\text{train}}^2 \right) - \sum_{t \in \text{incorrect}} \left(2\theta_{\text{train}} \cdot \epsilon_t^+ \cdot \bar{\epsilon}_{\text{train}} + \theta_{\text{train}}^2 \cdot \bar{\epsilon}_{\text{train}}^2 \right) \right) \\
 &\approx \frac{1}{N} \left(2\theta_{\text{train}} \cdot \bar{\epsilon}_{\text{train}} \cdot (n_{\text{train}}^{\text{correct}} \cdot \bar{\epsilon}_{\text{train}}) - n_{\text{train}}^{\text{correct}} \cdot \theta_{\text{train}}^2 \cdot \bar{\epsilon}_{\text{train}}^2 \right. \\
 &\quad \left. - 2\theta_{\text{train}} \cdot \bar{\epsilon}_{\text{train}} \cdot (n_{\text{train}}^{\text{incorrect}} \cdot \bar{\epsilon}_{\text{train}}) - n_{\text{train}}^{\text{incorrect}} \cdot \theta_{\text{train}}^2 \cdot \bar{\epsilon}_{\text{train}}^2 \right) \\
 &= (4\theta_{\text{train}} \cdot ACC_{\text{train}} - \theta_{\text{train}}^2 - 2\theta_{\text{train}}) \cdot \bar{\epsilon}_{\text{train}}^2, \tag{8}
 \end{aligned}$$

where ACC_{train} is the movement prediction accuracy on the training set, which is defined as:

$$ACC_{\text{train}} = \frac{n_{\text{train}}^{\text{correct}}}{n_{\text{train}}^{\text{incorrect}} + n_{\text{train}}^{\text{correct}}} \tag{9}$$

To maximize the value of $\Delta MSE_{\text{train}}$, we focus on the expression inside the parentheses of the final expression of Eq. (8) and regard it as a function of the parameter θ_{train} :

$$f(\theta_{\text{train}}) = 4\theta_{\text{train}} \cdot ACC_{\text{train}} - \theta_{\text{train}}^2 - 2\theta_{\text{train}} \tag{10}$$

Taking the derivative of $f(\theta_{\text{train}})$ and setting $f'(\theta_{\text{train}}) = 0$, the critical value of θ_{train} is as follows:

$$\theta_{\text{train}}^* = 2 \cdot ACC_{\text{train}} - 1 \tag{11}$$

Since $f''(\theta_{\text{train}}) < 0$, the function $f(\theta_{\text{train}})$ is concave downward, and the critical point of $f(\theta_{\text{train}})$ is a maximum. Correspondingly, θ_{train}^* represents the optimal parameter for FMNP determined via the training set. According to Eq. (11), θ_{train}^* is solely determined by ACC_{train} , indicating that ACC_{train} is the only factor influencing the fusion prediction on the training set. Given that when $ACC_{\text{train}} \in (0.5, 1)$, the movement prediction is meaningful, θ_{train}^* has a range between 0 and 1. According to Eqs. (8) and (11), the maximum improvement achieved by the fusion prediction over the naïve prediction on the training set is as follows:

$$\max \Delta MSE_{\text{train}} = (\theta_{\text{train}}^*)^2 \cdot \bar{\epsilon}_{\text{train}}^2 \tag{12}$$

2.3 Fusion on the test set

Suppose that θ_{train}^* and $\bar{\epsilon}_{\text{train}}$ are fed to Eq. (4) to generate the fusion prediction on the test set and the movement prediction on the test set with M time steps comprises $m_{\text{test}}^{\text{correct}}$ directions that are correct and $m_{\text{test}}^{\text{incorrect}}$ directions that are incorrect; then, the MSE difference between the naïve and fusion predictions on the test set can be expressed as follows:

$$\begin{aligned} \Delta MSE_{\text{test}} &= MSE_{\text{test}}^{\text{naïve}} - MSE_{\text{test}}^{\text{FMNP}} \\ &= \frac{1}{M} \left(\sum_{t \in \text{correct}} (\epsilon_t^+)^2 + \sum_{t \in \text{incorrect}} (\epsilon_t^+)^2 \right) - \frac{1}{M} \left(\sum_{t \in \text{correct}} \left((\epsilon_t^+)^2 - 2\theta_{\text{train}}^* \cdot \epsilon_t^+ \cdot \bar{\epsilon}_{\text{train}} + (\theta_{\text{train}}^*)^2 \cdot \bar{\epsilon}_{\text{train}}^2 \right) \right. \\ &\quad \left. + \sum_{t \in \text{incorrect}} \left((\epsilon_t^+)^2 + 2\theta_{\text{train}}^* \cdot \epsilon_t^+ \cdot \bar{\epsilon}_{\text{train}} + (\theta_{\text{train}}^*)^2 \cdot \bar{\epsilon}_{\text{train}}^2 \right) \right) \\ &= \frac{1}{M} \left(\sum_{t \in \text{correct}} \left(2\theta_{\text{train}}^* \cdot \epsilon_t^+ \cdot \bar{\epsilon}_{\text{train}} - (\theta_{\text{train}}^*)^2 \cdot \bar{\epsilon}_{\text{train}}^2 \right) - \sum_{t \in \text{incorrect}} \left(2\theta_{\text{train}}^* \cdot \epsilon_t^+ \cdot \bar{\epsilon}_{\text{train}} + (\theta_{\text{train}}^*)^2 \cdot \bar{\epsilon}_{\text{train}}^2 \right) \right) \end{aligned} \quad (13)$$

Similarly, on the basis of the LLN and that ϵ_t^+ is a positive random term, when both $m_{\text{test}}^{\text{correct}}$ and $m_{\text{test}}^{\text{incorrect}}$ are sufficiently large $\sum_{t \in \text{correct}} \epsilon_t^+$ approximates $m_{\text{test}}^{\text{correct}} \cdot \bar{\epsilon}_{\text{test}}$ and $\sum_{t \in \text{incorrect}} \epsilon_t^+$ approximates $m_{\text{test}}^{\text{incorrect}} \cdot \bar{\epsilon}_{\text{test}}$, where $\bar{\epsilon}_{\text{test}}$ is the true $\bar{\epsilon}$ of the test set. Accordingly, Eq. (13) can further be expressed as:

$$\begin{aligned} \Delta MSE_{\text{test}} &= MSE_{\text{test}}^{\text{naïve}} - MSE_{\text{test}}^{\text{FMNP}} \\ &\approx \frac{1}{M} \left(2\theta_{\text{train}}^* \cdot \bar{\epsilon}_{\text{train}} \cdot (m_{\text{test}}^{\text{correct}} \cdot \bar{\epsilon}_{\text{test}}) - m_{\text{test}}^{\text{correct}} \cdot (\theta_{\text{train}}^*)^2 \cdot \bar{\epsilon}_{\text{train}}^2 \right. \\ &\quad \left. - 2\theta_{\text{train}}^* \cdot \bar{\epsilon}_{\text{train}} \cdot (m_{\text{test}}^{\text{incorrect}} \cdot \bar{\epsilon}_{\text{test}}) - m_{\text{test}}^{\text{incorrect}} \cdot (\theta_{\text{train}}^*)^2 \cdot \bar{\epsilon}_{\text{train}}^2 \right) \\ &= 2\theta_{\text{train}}^* \cdot \bar{\epsilon}_{\text{train}} \cdot ACC_{\text{test}} \cdot \bar{\epsilon}_{\text{test}} - 2\theta_{\text{train}}^* \cdot \bar{\epsilon}_{\text{train}} \cdot (1 - ACC_{\text{test}}) \cdot \bar{\epsilon}_{\text{test}} - (\theta_{\text{train}}^*)^2 \cdot \bar{\epsilon}_{\text{train}}^2 \\ &= 2\theta_{\text{train}}^* \cdot \bar{\epsilon}_{\text{train}} \cdot \theta_{\text{test}}^* \cdot \bar{\epsilon}_{\text{test}} - (\theta_{\text{train}}^*)^2 \cdot \bar{\epsilon}_{\text{train}}^2, \end{aligned} \quad (14)$$

where ACC_{test} is the movement prediction accuracy on the test set, which is defined as:

$$ACC_{\text{test}} = \frac{m_{\text{test}}^{\text{correct}}}{m_{\text{test}}^{\text{incorrect}} + m_{\text{test}}^{\text{correct}}}, \quad (15)$$

and θ_{test}^* is the optimal weight that controls the magnitude of the increments for the fusion on the test set, which is derived by:

$$\theta_{\text{test}}^* = 2 \cdot ACC_{\text{test}} - 1 \quad (16)$$

According to Eq. (14), if the fusion prediction is superior to the naïve prediction, ΔMSE_{test} should be greater than zero. Therefore, the following inequality should be fulfilled:

$$\theta_{\text{test}}^* \cdot \bar{\epsilon}_{\text{test}} > \frac{1}{2} \theta_{\text{train}}^* \cdot \bar{\epsilon}_{\text{train}} \quad (17)$$

However, the values of the independent variables θ_{test}^* and $\bar{\epsilon}_{\text{test}}$ cannot be known in advance. Assuming that θ_{train}^* and $\bar{\epsilon}_{\text{train}}$ follow distributions with positive value ranges, if we regard θ_{train}^* and $\bar{\epsilon}_{\text{train}}$ as the estimations for θ_{test}^* and $\bar{\epsilon}_{\text{test}}$, then the probability of satisfying inequality (17) can be expressed as:

$$P \left(\theta_{\text{test}}^* \cdot \bar{\epsilon}_{\text{test}} > \frac{1}{2} \theta_{\text{train}}^* \cdot \bar{\epsilon}_{\text{train}} \right) \quad (18)$$

To maximize this probability, the estimations of θ_{test}^* and $\bar{\epsilon}_{\text{test}}$ should be as small as possible. However, if the product of the two estimations is too close to zero, the improvement in the fusion over the naïve prediction on the test set will also diminish. Therefore, setting the estimations of θ_{test}^* and $\bar{\epsilon}_{\text{test}}$ involves a trade-off between maximizing the probability of the FMNP method outperforming the naïve prediction and ensuring sufficient improvement.

A practical method for determining the estimations of θ_{test}^* and $\bar{\epsilon}_{\text{test}}$ is outlined as follows. Consider a data generating process where a sliding window, with a length equal to that of the test set, moves sequentially from the beginning to the end of the training set. The data points in each window can be treated as a "test set" in the historical context. Within each window, the movement prediction accuracy is calculated, generating a corresponding θ value via Eq. (11). Consequently, a set of θ values, denoted as Θ_{set} , is generated through this process, the bounds of which can be regarded

as a value range of θ_{test}^* . Similarly, a sliding window of the same length is used to calculate a set of $\bar{\epsilon}$ values from the training set, denoted as $\bar{\epsilon}_{\text{set}}$, providing a value range of the $\bar{\epsilon}_{\text{test}}$ based on historical data.

Consider a set consisting of θ values derived from nonoverlapping windows that construct the whole training set, denoted as $\Theta_{\text{non-ovlp}}$, $\Theta_{\text{non-ovlp}} \subset \Theta_{\text{set}}$; then, θ_{train}^* can be expressed as the expected value of this set:

$$\theta_{\text{train}}^* = \mathbb{E}(\Theta_{\text{non-ovlp}}) \quad (19)$$

Similarly, $\bar{\epsilon}_{\text{train}}$ can be expressed as the expected value of the set $\bar{\epsilon}_{\text{non-ovlp}}$:

$$\bar{\epsilon}_{\text{train}} = \mathbb{E}(\bar{\epsilon}_{\text{non-ovlp}}), \quad (20)$$

where $\bar{\epsilon}_{\text{non-ovlp}}$ represents the $\bar{\epsilon}$ values derived from the same nonoverlapping windows and where $\bar{\epsilon}_{\text{non-ovlp}} \subset \bar{\epsilon}_{\text{set}}$. Since $\mathbb{E}(\Theta_{\text{non-ovlp}}) \geq \min(\Theta_{\text{set}})$ and $\mathbb{E}(\bar{\epsilon}_{\text{non-ovlp}}) \geq \min(\bar{\epsilon}_{\text{set}})$, we have:

$$\theta_{\text{train}}^* \geq \min(\Theta_{\text{set}}), \bar{\epsilon}_{\text{train}} \geq \min(\bar{\epsilon}_{\text{set}}), \quad (21)$$

where $\Theta_{\text{set}(\min)}$ and $\bar{\epsilon}_{\text{set}(\min)}$ are the minimum values from the respective Θ_{set} and $\bar{\epsilon}_{\text{set}}$. Suppose that the movement prediction accuracy for each sliding window exceeds 0.50 or that each element in Θ_{set} is greater than zero. In that case, we can use $\min(\Theta_{\text{set}})$ and $\min(\bar{\epsilon}_{\text{set}})$ as the estimations of θ_{test}^* and $\bar{\epsilon}_{\text{test}}$ and feed them into Eq. (4) to increase the probability of the FMNP outperforming the naive prediction. Consequently, the fusion prediction for each future time step can be adjusted as:

$$\hat{y}_t = y_{t-1} + \hat{D}_t \cdot \min(\Theta_{\text{set}}) \cdot \min(\bar{\epsilon}_{\text{set}}) \quad (22)$$

Accordingly, the whole fusion prediction on the test set can be derived via Algorithm 1.

2.4 Movement Prediction with an Exogenous Variable

The FMNP method presupposes that movement predictions have consistent accuracies greater than 0.50 across different subsets, which indicates that the movement prediction accuracy should be above 0.50 for all the sliding windows. However, achieving consistent movement prediction accuracy across different subsets is challenging in practice, as the forecasting model is often susceptible to overfitting or underfitting, which results in inconsistent performance (Aliferis & Simon, 2024; Montesinos López et al., 2022). Moreover, the movement predictions on the test set frequently exhibit a trivial nature, whereby the model becomes biased toward predicting the majority class, although such predictions can often achieve an accuracy above 0.50 (Drummond & Holte, 2005; Josephine, 2017).

This study proposes a practical approach to generate movement predictions, which leverages the comovement between the target variable and an exogenous variable and serves as an auxiliary tool for applying FMNP in real forecasting tasks. The selection of the exogenous variable is typically guided by domain knowledge, and the movement prediction of the target variable, denoted as $\hat{D}_t^{\text{target}}$, can be simply obtained as:

$$\hat{D}_t^{\text{target}} = \hat{D}_t^{\text{exo}}, \quad (23)$$

where \hat{D}_t^{exo} represents the movement prediction of the exogenous variable at time step t . In particular, if the value of the exogenous variable is recorded early enough relative to the target variable at the same time step, such as in financial markets with different trading hours across time zones, its actual movement can be directly used as the movement prediction for the target variable:

$$\hat{D}_t^{\text{target}} = D_t^{\text{exo}} = \begin{cases} 1, & \text{if } y_t^{\text{exo}} > y_{t-1}^{\text{exo}}; \\ -1, & \text{if } y_t^{\text{exo}} \leq y_{t-1}^{\text{exo}}; \end{cases} \quad (24)$$

where D_t^{exo} is the actual movement of the target variable at time step t . For each sliding window, the movement prediction accuracy of the target variable can be obtained as follows:

$$ACC_{\text{sliding window}} = \frac{1}{n} \sum_{i=1}^n 1(D_i^{\text{exo}} = D_i^{\text{target}}), \quad (25)$$

where n is the total number of time steps in each sliding window and D_i^{exo} and D_i^{target} are the i th actual movements of the exogenous and target variables within each window, respectively. $1(D_i^{\text{exo}} = D_i^{\text{target}})$ is an indicator function that equals 1 if the movement prediction of the exogenous variable matches the movement prediction of the target variable and 0 otherwise. If the movement prediction accuracy is not greater than a predefined threshold (e.g., 0.51), the exogenous variable is considered unsuitable for reliable movement prediction, and a new variable should be selected for evaluation. This cyclical process ensures that only accurate and robust movement predictions of the target variable are provided to ensure the FMNP's effectiveness.

Algorithm 1 FMNP On Test Set**Inputs:** Y_{train} : Array of observations in the training set Y_{test} : Array of observations in the test set \hat{D}_{train} : Array of movement prediction corresponding to the training set \hat{D}_{test} : Array of movement prediction corresponding to the test set N : Number of elements in the training set M : Number of elements in the test set**Output:** P : Array of fusion results for the test set**1.** Initialize the variables for the movement, prediction, and tracking metrics: $D_{\text{train}} \leftarrow []$ // Array for actual movements in the training set $P \leftarrow []$ // Array for final fusion predictions in the test set $ACC_{\text{set}} \leftarrow []$ // Array of movement prediction accuracies for the sliding windows $\Theta_{\text{set}} \leftarrow []$ // Array of weights for the sliding windows $R_{\text{train}} \leftarrow []$ // Array of first-order differences for the training set $\bar{\epsilon}_{\text{set}} \leftarrow []$ // Array of mean absolute increments for the sliding windows**2.** Calculate the actual movements for the training set:**for** $t \leftarrow 1$ to $\text{length}(Y_{\text{train}})$ **do** $\text{diff} \leftarrow Y_{\text{train}}[t] - Y_{\text{train}}[t - 1]$ // Calculate first-order difference $R_{\text{train}}.\text{append}(\text{diff})$ **if** $\text{diff} > 0$ **then** $D_{\text{train}}.\text{append}(1)$ // Upward movement **else** $D_{\text{train}}.\text{append}(-1)$ // Downward or no movement **end if****end for****3.** Calculate the movement prediction accuracies for the sliding windows:**for** $t \leftarrow 1$ to $N - M + 1$ **do** $\text{Correct_Predictions} \leftarrow 0$ **for** $i \leftarrow t$ to $t + M - 1$ **do** **if** $D_{\text{train}}[i] == \hat{D}_{\text{train}}[i]$ **then** $\text{Correct_Predictions} \leftarrow \text{Correct_Predictions} + 1$ **end if** **end for** $ACC_{\text{set}}.\text{append}(\text{Correct_Predictions}/M)$ // Append accuracy for the current window**end for****4.** Compute Θ_{set} for the sliding windows:**for each** $ACC \in ACC_{\text{set}}$ **do** $\theta \leftarrow 2 \cdot (ACC - 1)$ // Calculate weight for movement contribution $\Theta_{\text{set}}.\text{append}(\theta)$ **end for****5.** Calculate $\bar{\epsilon}_{\text{set}}$ for the sliding windows:**for** $t \leftarrow 1$ to $(N - M + 1)$ **do** $\bar{\epsilon} \leftarrow \text{mean}(\text{abs}(R_{\text{train}}[t : t + M - 1]))$ // Mean absolute increment for each sliding window $\bar{\epsilon}_{\text{set}}.\text{append}(\bar{\epsilon})$ **end for****6.** Set the initial forecast value: $Y_{\text{last}} \leftarrow Y_{\text{train}}[\text{end}]$ // Use the last training set value as the starting point**7.** Generate fusion predictions for the test set:**for** $i \leftarrow 1$ to $\text{length}(Y_{\text{test}})$ **do** $\Delta \leftarrow \min(\Theta_{\text{set}}) \cdot \min(\bar{\epsilon}_{\text{set}}) \cdot \hat{D}_{\text{test}}[i]$ // Compute increment $Y_{\text{forecast}} \leftarrow Y_{\text{last}} + \Delta$ // Calculate fusion forecast for each time step $P.\text{append}(Y_{\text{forecast}})$ // Store forecast $Y_{\text{last}} \leftarrow Y_{\text{test}}[i]$ // Update for the next prediction**end for****8.** Return P

3 Simulation

This section presents a simulation study using synthetic data to evaluate whether FMNP outperforms naïve prediction at specific accuracy levels. Given the movement prediction accuracy for the test set, the simulation examines scenarios with differing movement predictions but identical accuracy to statistically test FMNP performance.

3.1 Datasets and Setup

The synthetic dataset encompasses symmetric random walks with diverse types of variance to ensure comprehensive testing. The types of variance include constant variance and varying variance, with the latter comprising linear variance trends representing gradual changes over time, cyclic or seasonal variance introducing periodic patterns, and randomly varying variance reflecting stochastic behavior, as summarized in Table 1.

Table 1: Synthetic data summary

Variance Type	Expression	Parameter Range
Constant variance	$\sigma_t^2 = \sigma_0^2$	$\sigma_0^2 = 1$
Linear variance trend	$\sigma_t^2 = \frac{\sigma_0^2}{1+k \cdot t}$	$\sigma_0^2 = 1, k \in (0, 10)$
Cyclic variance	$\sigma_t^2 = \sigma_0^2(1 + a \cdot \sin(\omega t))$	$\sigma_0^2 = 1, \omega = \frac{2\pi}{100}, a \in (0, 10)$
Randomly varying variance	$\sigma_t^2 = \sigma_{t-1}^2 + \eta_t, \eta_t \sim \mathcal{N}(0, \xi^2)$	$\sigma_0^2 = 1, \xi^2 \in (0, 1000)$

Accordingly, four synthetic time series were generated, as shown in Figure 1. Each time series, consisting of 2,500 steps, was generated in the Python environment. For each type of random walk, the parameters are randomly selected once from the range provided in Table 1, using a fixed random seed (seed = 1). To maintain all the values within a positive range, an initial positive offset of 10000 units was applied to each series. The last 500 data points were selected as the test set, whereas the remaining data points were used as the training set.

For each time series, the fusion result was generated via Algorithm 1, which uses values of θ determined by different levels of predefined movement prediction accuracies. The performance of each fusion result was evaluated via four metrics: RMSE, MAE, MAPE, and sMAPE. The RMSE, derived from the square root of the MSE, emphasizes larger errors, making it suitable for identifying significant deviations in forecasts. The MAE, on the other hand, provides an interpretable measure of average error without overpenalizing outliers. The MAPE and sMAPE normalize errors relative to actual values, enabling comparisons across datasets with different scales. Together, these metrics capture both absolute and relative error characteristics, ensuring a robust and balanced evaluation. The formulas for these metrics are as follows:

$$RMSE = \sqrt{\frac{1}{N} \sum_{i=1}^N (y_i - \hat{y}_i)^2}, \quad (26)$$

$$MAE = \frac{1}{N} \sum_{i=1}^N |y_i - \hat{y}_i|, \quad (27)$$

$$MAPE = \frac{100}{N} \sum_{i=1}^N \left| \frac{y_i - \hat{y}_i}{y_i} \right|, \quad (28)$$

$$sMAPE = \frac{100}{N} \sum_{i=1}^N \frac{|y_i - \hat{y}_i|}{\frac{|y_i| + |\hat{y}_i|}{2}}, \quad (29)$$

where N denotes the test set size, \hat{y}_i denotes the predicted value, and y_i denotes the actual value. To statistically test the performance of FMNP, for each synthetic time series at a specified accuracy level, the fusion process was repeated 100 times. Each repetition used a unique movement prediction sequence at the same accuracy level, generated by randomly replacing a subset of actual movements in the test set with incorrect movements. The accuracy level is adjusted in two stages: initially, it changes from 0.50 to 0.56 in increments of 0.01, and then it changes from 0.55 to 1.00 in larger increments of 0.05. This approach allows for finer granularity in the lower accuracy range, where small changes can have a significant effect on performance, while using larger steps at higher accuracy levels balances computational efficiency. Consequently, for each synthetic time series, 100 independent values of each metric were calculated at each accuracy level.

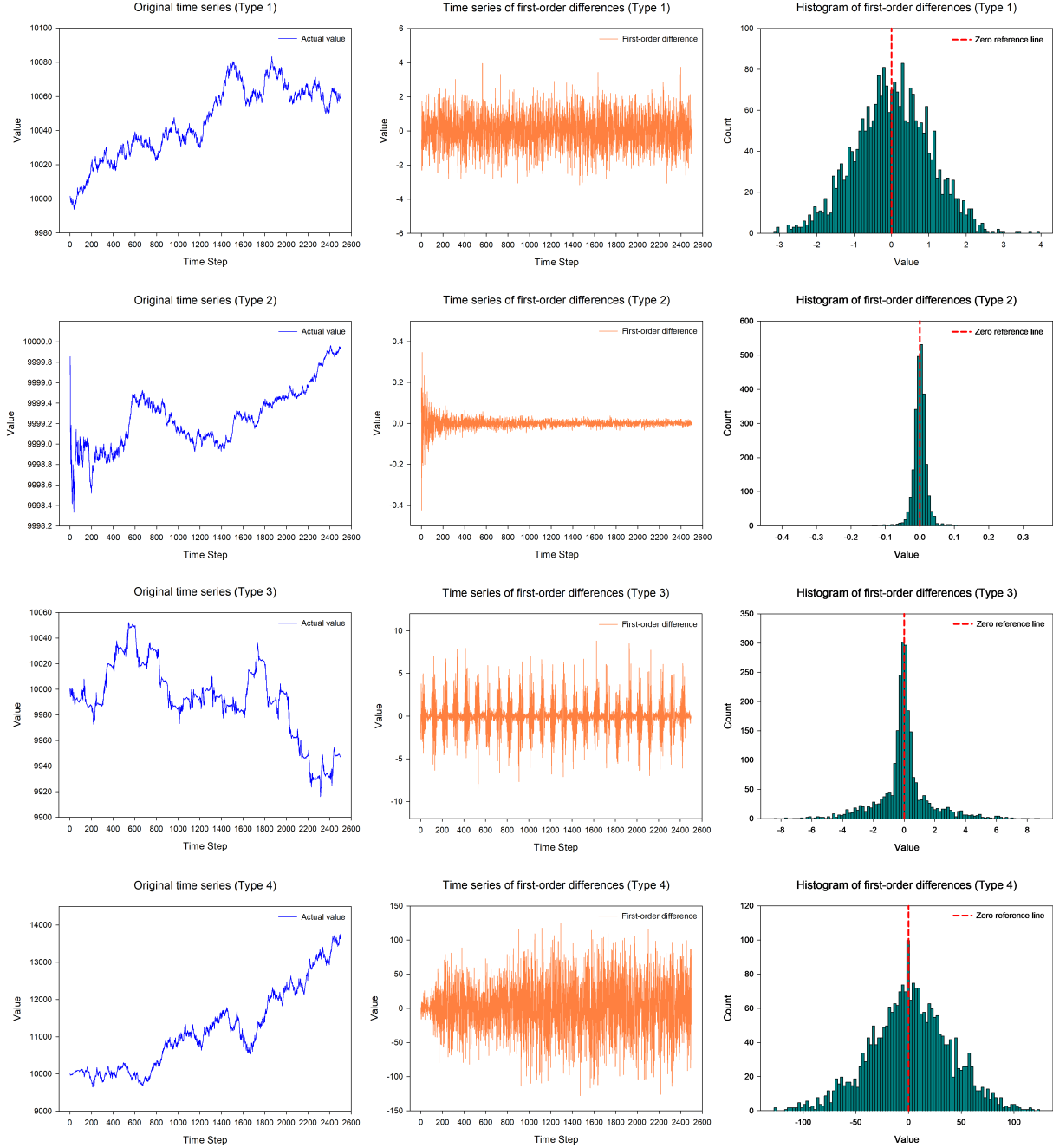


Figure 1: Synthetic time series: Type 1, constant variance ($\sigma_0^2 = 1$); Type 2, linear variance trend ($k = 4.95$); Type 3, cyclic variance ($a = 7.77$); and Type 4, randomly varying variance ($\xi^2 = 920$).

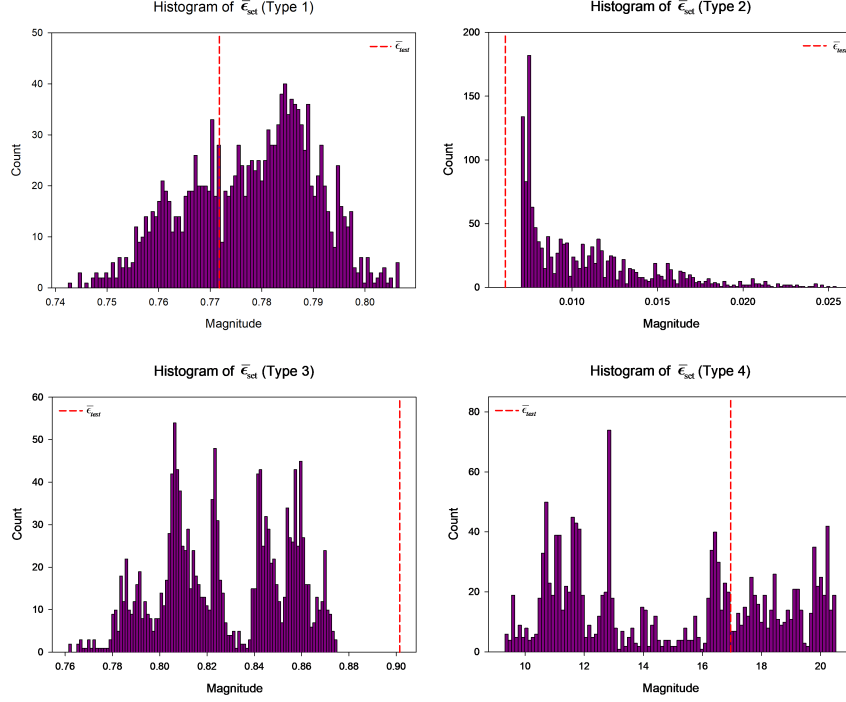


Figure 2: Comparison of the true $\bar{\epsilon}_{test}$ with $\bar{\epsilon}_{set}$: Type 1, constant variance ($\sigma_0^2 = 1$); Type 2, linear variance trend ($k = 4.95$); Type 3, cyclic variance ($a = 7.77$); and Type 4, randomly varying variance ($\xi^2 = 920$).

3.2 Results and Analysis

Since the movement prediction accuracy for the test set is predefined in each simulation process, only $\bar{\epsilon}_{test}$ must be estimated. Figure 2 illustrates the distribution of the values in the $\bar{\epsilon}_{set}$, generated on the basis of sliding windows across the first-order differences of the training set. The vertical reference line in Figure 2 represents the true $\bar{\epsilon}_{test}$ of the test set. According to Eq. (22), $\min(\bar{\epsilon}_{set})$ serves as the estimate for $\bar{\epsilon}_{test}$. In the four cases, the minimum value from $\bar{\epsilon}_{set}$ is generally an underestimation of $\bar{\epsilon}_{test}$, except for the second case, where the synthetic time series is a random walk with a decreasing linear variance trend. Nonetheless, the estimated value remains close to the true value. Under the assumption that movement prediction accuracy is consistent across the training and test sets, this estimation ensures that the inequality (17) is satisfied.

Furthermore, the comparisons of fusion prediction with naïve prediction at low accuracy levels and high accuracy levels are illustrated in Figures 3 and 4, respectively. Within each figure, each box plot represents the distribution of 100 independent metric values at a specific accuracy level, with the metric value of the naïve prediction shown as a reference line. According to Figure 3, at lower accuracy levels, such as 0.51, the RMSE of the FMNP method is comparable to or slightly better than that of the naïve prediction, as shown by the proximity of the median of each box plot to the reference line, which represents the naïve RMSE. As the accuracy increases beyond 0.52, the majority of the RMSE values fall below the baseline.

According to Figure 4, at higher accuracy levels ranging from 0.55 to 1.00, the FMNP method consistently outperforms the naïve prediction across nearly all trials. Notably, the improvement over the naïve prediction becomes more pronounced as the movement prediction accuracy improves, with enhancements of approximately 30% for certain metrics. This finding demonstrates that highly accurate movement predictions can be effectively translated into improved point forecasts in the context of random walk forecasting. However, the performance of the FMNP method has boundaries, as it allows random walks to be predicted to a certain extent but is not infinitely close to the true value.

Since the FMNP method consistently outperforms the naïve baseline in terms of the MAE, MAPE, and sMAPE comparisons, the one-sample Wilcoxon signed-rank test was conducted to specifically evaluate whether the median differences between the RMSE values of the FMNP forecasts and those of the naïve predictions significantly deviated from zero for accuracy levels ranging from 0.50 to 0.56 (Li & Johnson, 2014). As summarized in Table 2, at the accuracy level of 0.51, the FMNP method shows mixed results regarding statistical significance. While significant

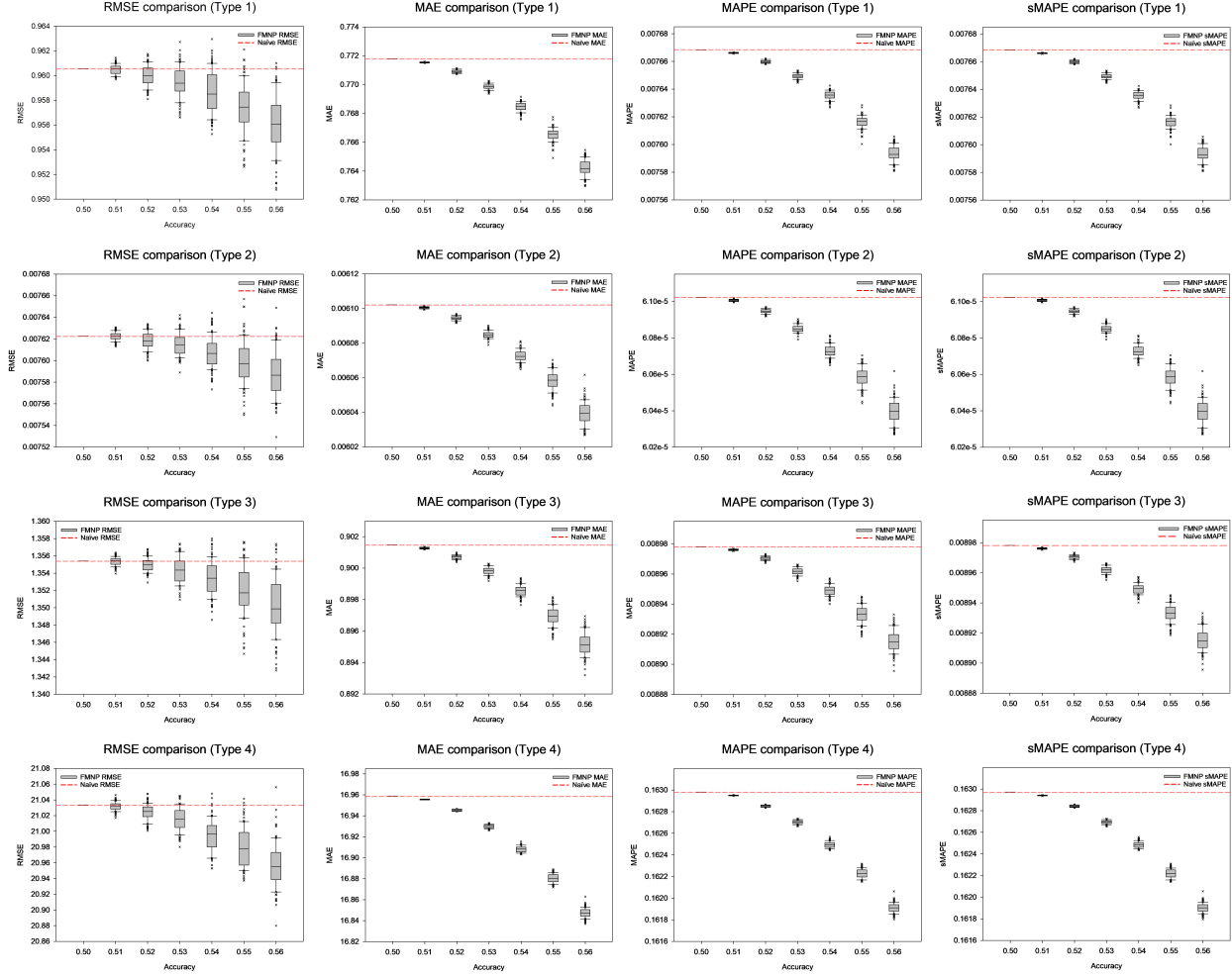


Figure 3: Summary of the fusion predictions across different accuracy levels (0.50–0.56) for four types of random walks: Type 1, constant variance; Type 2, linear variance trend; Type 3, cyclic variance; and Type 4, randomly varying variance.

improvements over the naïve baseline are observed for Type 4 (randomly varying variance, $p = 0.002$), the results for Type 1 (constant variance, $p = 0.915$), Type 2 (linear variance trend, $p = 0.781$), and Type 3 (cyclic variance, $p = 0.812$) are not statistically significant, indicating that an accuracy level of 0.51 may not consistently yield meaningful improvements across all types. As the accuracy increases beyond 0.51, significant reductions in the RMSE ($p < 0.001$) are observed for all types, demonstrating the FMNP method’s reliability and effectiveness at higher accuracy levels. Therefore, an accuracy level of 0.51 must be exceeded for the FMNP method to be effective and surpass the naïve baseline in practice.

In general, when the movement prediction accuracy equals 0.5, the fusion process provides no improvement over the naïve prediction. However, as the movement prediction accuracy increases, the performance of the fusion prediction improves. This performance of FMNP under different accuracy levels, demonstrated across four representative synthetic time series, underscores its robustness and potential applicability to a wide range of symmetric random walks, including those with homoscedasticity as well as high-volatility scenarios.

4 Real-world Experiments

This section evaluates the performance of the FMNP method on real-world data. It includes a description of the datasets, details of the experimental setup, and a comparative analysis of the FMNP method’s performance against the naïve baseline.

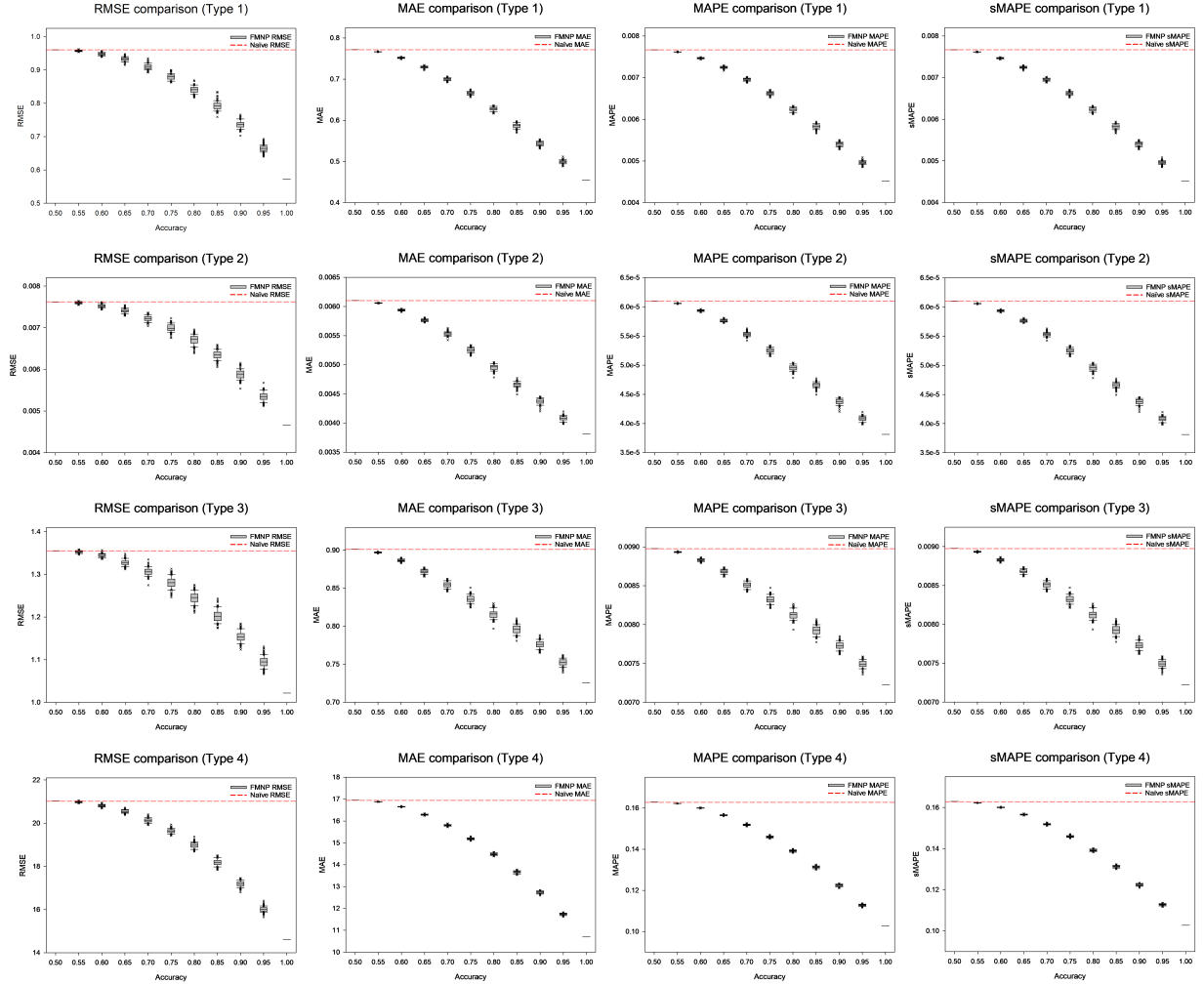


Figure 4: Summary of the fusion predictions across different accuracy levels (0.55–1.00) for four types of random walks: Type 1, constant variance; Type 2, linear variance trend; Type 3, cyclic variance; and Type 4, randomly varying variance.

Table 2: RMSE results of the fusion predictions across accuracy levels (0.50–0.56) for four types of random walks: Type 1, constant variance; Type 2, linear variance trend; Type 3, cyclic variance; and Type 4, randomly varying variance.

Prediction	Type 1		Type 2		Type 3		Type 4	
	RMSE Range	p-value	RMSE Range	p-value	RMSE Range	p-value	RMSE Range	p-value
Naïve	0.961	-	0.00762	-	1.355	-	21.034	-
Acc = 0.50	0.961	-	0.00762	-	1.355	-	21.034	-
Acc = 0.51	0.960 ± 0.0004	0.915	0.00762 ± 0.000003	0.781	1.355 ± 0.0005	0.812	21.032 ± 0.0053	0.002
Acc = 0.52	0.960 ± 0.0008	<0.001	0.00762 ± 0.000007	<0.001	1.355 ± 0.0008	<0.001	21.024 ± 0.0102	<0.001
Acc = 0.53	0.959 ± 0.0012	<0.001	0.00761 ± 0.000010	<0.001	1.354 ± 0.0015	<0.001	21.015 ± 0.0144	<0.001
Acc = 0.54	0.959 ± 0.0017	<0.001	0.00761 ± 0.000014	<0.001	1.353 ± 0.0020	<0.001	20.995 ± 0.0199	<0.001
Acc = 0.55	0.957 ± 0.0020	<0.001	0.00760 ± 0.000020	<0.001	1.352 ± 0.0028	<0.001	20.979 ± 0.0244	<0.001
Acc = 0.56	0.956 ± 0.0023	<0.001	0.00758 ± 0.000021	<0.001	1.351 ± 0.0032	<0.001	20.957 ± 0.0278	<0.001

Table 3: Statistics of five financial time series.

Time series	Date	Count	Mean	Std. Dev.	Minimum	Median	Maximum
BA (Close price)	10.08.2014 - 09.13.2024	2500	211.23	80.88	95.01	195.92	430.30
OIL (Close price)	10.08.2014 - 09.13.2024	2500	66.42	18.58	19.33	65.20	127.98
HAL (Close price)	10.08.2014 - 09.13.2024	2500	30.98	9.60	4.32	33.30	50.52
SLB (Close price)	10.08.2014 - 09.13.2024	2500	45.93	15.44	11.02	49.49	74.91
FTSE (Open price)	10.08.2014 - 09.13.2024	2500	7092.18	592.35	4993.90	7210.0	8445.80

Table 4: Examination results for the training sets of four financial time series.

Time series	ADF Statistic	ADF p-value	Mean of First Differences	t-statistic	t-test p-value	ARCH Statistic	ARCH p-value
BA	-1.6700	0.4466	0.0002	0.1776	0.8590	1956.1220	0.0000
OIL	-2.0765	0.2541	-0.0000	-0.0015	0.9988	1930.1919	0.0000
HAL	-2.2270	0.1966	-0.0011	-0.7067	0.4798	1957.3615	0.0000
SLB	-1.8049	0.3780	-0.0011	-0.9226	0.3563	1961.3134	0.0000

4.1 Datasets and Setup

For demonstration purposes, real-world datasets are selected on the basis of whether the time series of the target variable can be regarded as a symmetric random walk and whether there exists an exogenous variable exhibiting comovement with it. On the basis of these criteria, four financial time series in the U.S. market, including the close prices of Boeing Company (BA), Brent crude oil (OIL), Halliburton Company (HAL), and Schlumberger Limited (SLB), are selected as the forecasting targets, and the open price of the Financial Times Stock Exchange (FTSE) index is employed as the exogenous variable, given that strong comovement has been observed between the FTSE index and the U.S. stock market indices (Gupta et al., 2024; Sarwar, 2020). Owing to the differing operational times of the stock exchanges, the open price of FTSE is recorded 13 hours before the close prices of the financial time series from the U.S. markets on the same date; therefore, according to Eq. (24), the actual movement of the FTSE open price can be used as the movement prediction for the closing prices in the U.S. markets at the same time step.

The raw data of the five real-world financial time series were retrieved from Yahoo Finance, covering the period from October 8, 2014, to September 13, 2024. The raw data of FTSE were aligned with the other four datasets on a day-by-day basis, with any additional data points removed and missing values filled via forward filling (Junninen et al., 2004). Following the alignment of the data, each dataset has a length of precisely 2,500 time steps. The first 2000 data points of each dataset were allocated as the training set, whereas the remaining points served as the test set. All the close prices of the four target variables, as well as the open price of FTSE, are shown in Figure 5 and Figure 6, respectively, and are briefly described in Table 3.

To determine whether the four time series—BA, OIL, HAL, and SLB—follow a random walk, the augmented Dickey-Fuller (ADF) test and the autoregressive conditional heteroskedasticity (ARCH) test were conducted on the training set data. As shown in Table 4, the ADF test results reveal p values above 0.05 for all series, indicating that the null hypothesis of a unit root cannot be rejected. This supports the classification of these time series as random walks. Additionally, the ARCH test results demonstrate strong evidence of heteroskedasticity, with extremely high ARCH statistics and p values of 0.0000 across all series.

According to the second and third columns of Figure 5, the first-order differences of the four time series exhibit approximately symmetric distributions centered around zero. This observation is supported by the results in Table 4, where the means of the first differences are close to zero for all series. The t tests conducted on the first-order differences yield t statistics near zero and p values well above 0.05, confirming that the mean differences do not significantly deviate from zero. These results confirm the symmetric nature of the first-order differences, further highlighting the symmetric properties of the four financial time series.

The fusion prediction on the test set for each financial time series is generated via Algorithm 1, with the naïve prediction as the sole baseline. This choice is justified because there is no strong evidence that complex methods, such as machine learning or deep learning-based models, can consistently outperform naïve prediction in forecasting real-world time series that exhibit the characteristics of symmetric random walks (Jadecivicius & Huston, 2015; Rogers, 1995). In fact, naïve prediction often serves as a strong baseline in random walk forecasting, as many sophisticated models struggle to provide significant improvements over it.

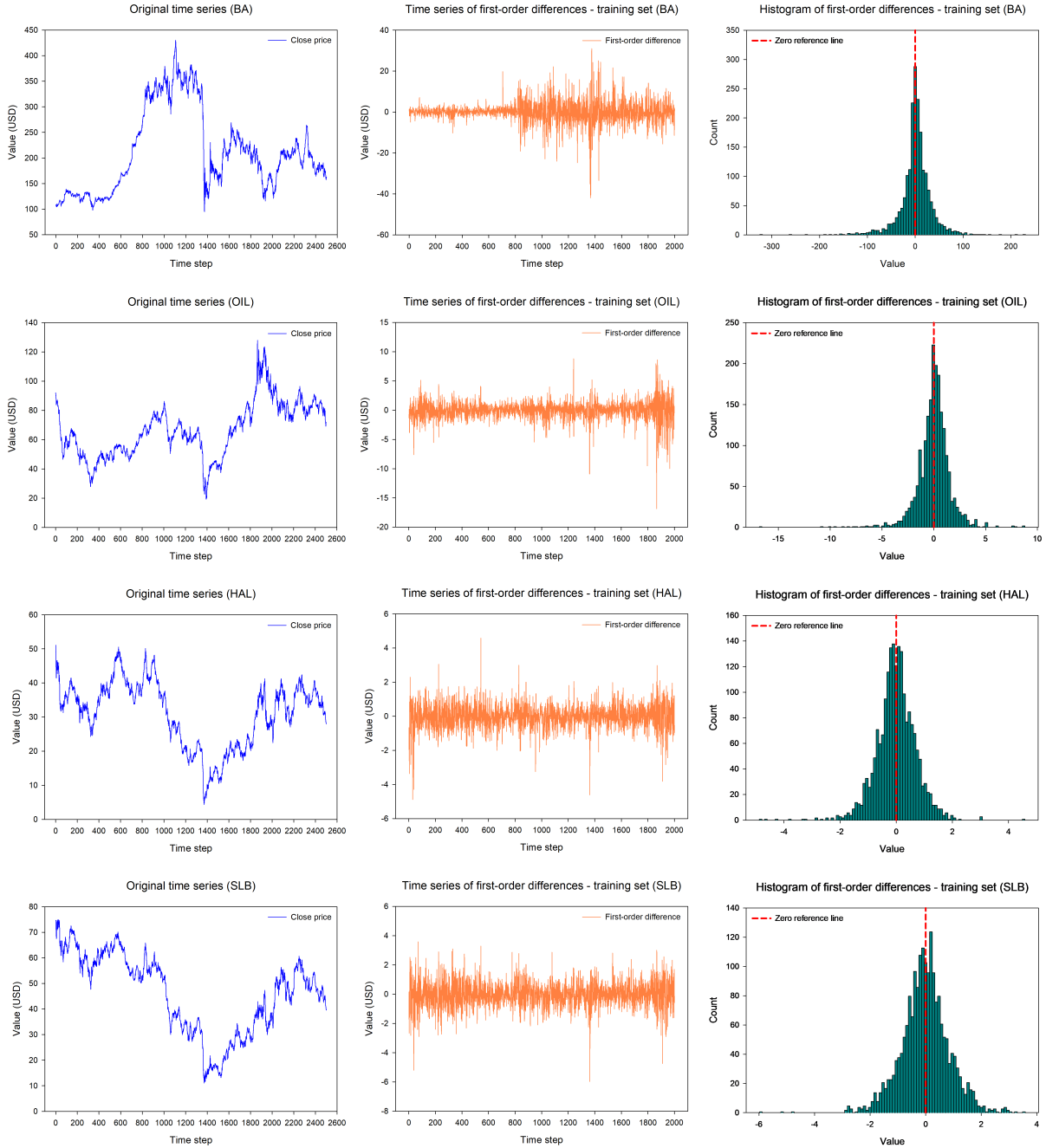


Figure 5: Time series of four target variables.

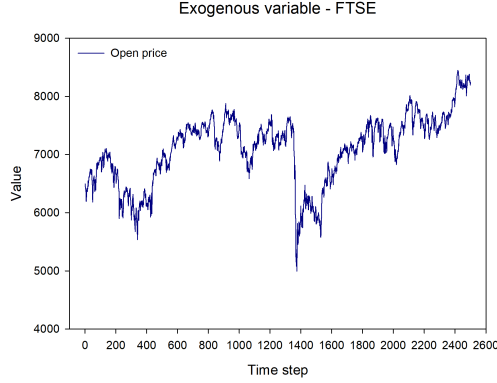


Figure 6: Open price of FTSE.

To evaluate the performance of the FMNP method, the same four metrics used in the simulation experiments—the RMSE, MAE, MAPE, and sMAPE—are employed. These metrics provide a comprehensive framework for assessing absolute and relative errors, enabling a robust comparison with the naïve baseline.

4.2 Results and Analysis

The forecasting results for four financial time series using different methods are shown in Figure 7. The first column of Figure 7 displays the distribution of movement prediction accuracy obtained from sliding windows on the training set, with a reference line indicating the true movement prediction accuracy on the test set. The minimum value of each accuracy set serves as an estimation of the true accuracy. Among the datasets, the BA and HAL cases reveal that even the minimum value of the accuracy set is an overestimation of the true accuracy on the test set. This highlights the variability in movement prediction, even when the exogenous variable has strong comovement with the target variable. Nonetheless, the movement prediction accuracy across the sliding windows of the training set consistently exceeds 0.51, which is the threshold required to ensure the effectiveness of FMNP.

The second column of Figure 7 illustrates the distribution of $\bar{\epsilon}$ values computed by sliding windows on the training set, with a reference line representing the true $\bar{\epsilon}$ of the test set. In all four cases, the true $\bar{\epsilon}$ lies within the range of $\bar{\epsilon}_{\text{set}}$. Consequently, the minimum $\bar{\epsilon}$ value for each case underestimates the true value of $\bar{\epsilon}_{\text{test}}$. Except under extreme conditions in the test set, such as periods of exceptionally high volatility or a complete lack of volatility, the estimation of $\bar{\epsilon}_{\text{test}}$ via $\min(\bar{\epsilon}_{\text{set}})$ usually will not overestimate the true $\bar{\epsilon}_{\text{test}}$. This ensures a high probability that the fusion prediction will outperform the naïve baseline, as indicated by Eq. (18).

The third column of Figure 7 presents the predictions of the FMNP method and the naïve predictions for the last ten points of the test set. Minor discrepancies between the two methods are observed, primarily due to low estimated values of movement prediction accuracy and $\bar{\epsilon}_{\text{test}}$. In the case of SLB forecasting, the estimated accuracy was 0.526, whereas the true movement prediction accuracy was 0.552. Consequently, the estimated θ_{test}^* was 0.052, whereas the true value was 0.104. According to Eq. (14), even if the estimation of $\bar{\epsilon}_{\text{test}}$ is accurate, a low estimation of θ_{test}^* in this case leads to the final improvement being only 75% of the ideal fusion result.

Table 5 provides a performance comparison between the FMNP method and the naïve prediction across the four target datasets. The FMNP method consistently outperforms the naïve prediction, albeit with marginal differences. It achieves lower RMSE and MAE values, demonstrating improved accuracy in terms of absolute error terms. Additionally, the FMNP method results in slight reductions in the MAPE and sMAPE, reflecting better relative error performance. These findings suggest that the FMNP method effectively refines predictions even in scenarios with low movement prediction accuracy. The results highlight the ability of the FMNP method to increase forecast accuracy, its superiority over naïve prediction, and its generalizability across diverse forecasting scenarios.

The findings from real-world experiments align with prior analyses, where the estimation for θ_{test}^* and $\bar{\epsilon}_{\text{test}}$ represents a trade-off: smaller estimated values increase the probability of the fusion prediction surpassing the naïve prediction but limits the magnitude of improvement. Overall, the adjusted fusion according to Eq. (22) effectively balances these factors, providing a reliable enhancement over the naïve baseline, even under challenging conditions.

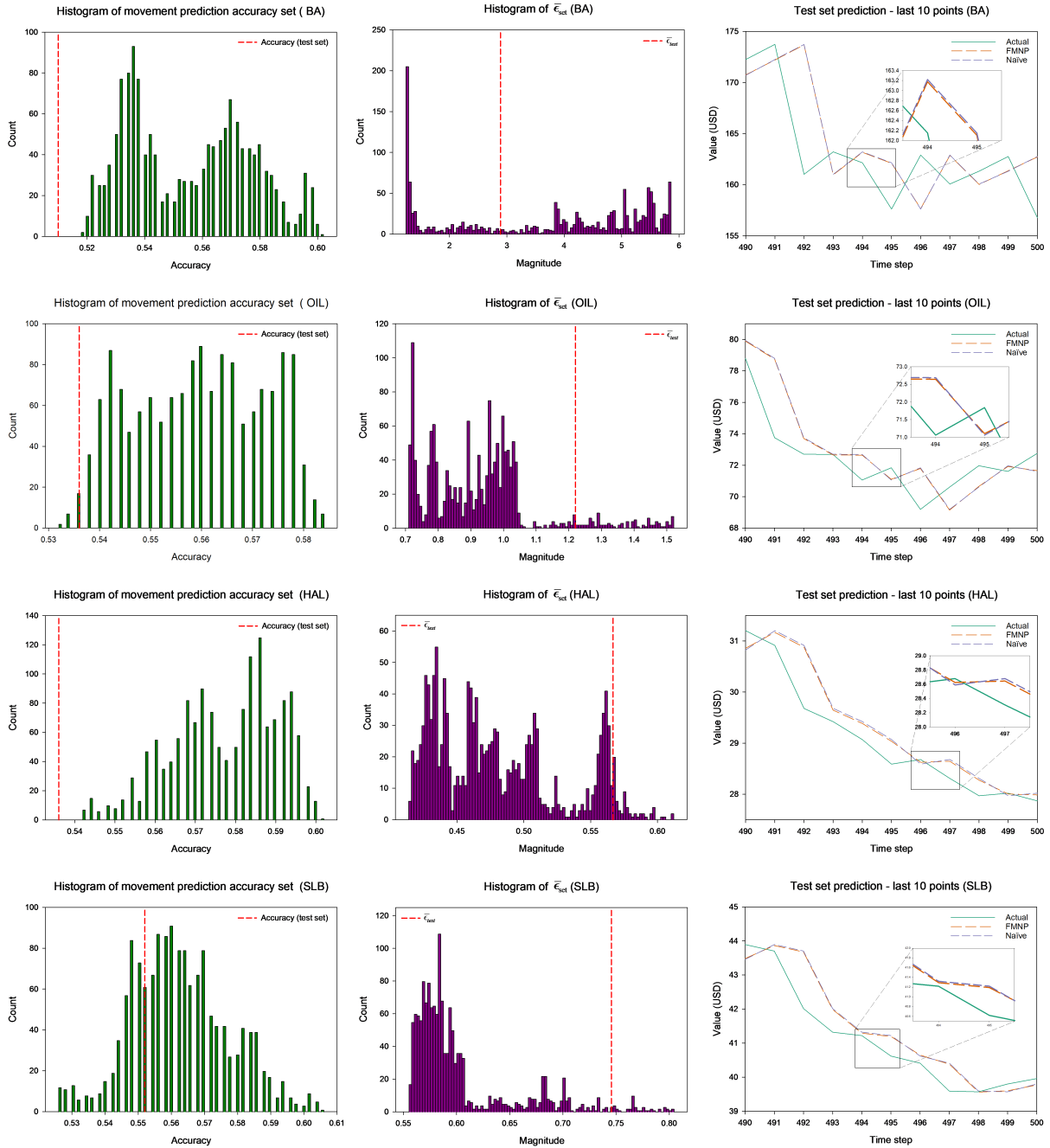


Figure 7: Four financial time series forecasting results.

Table 5: Performance comparison of the FMNP method and the naïve prediction on various target datasets.

Target	Model	RMSE	MAE	MAPE (%)	sMAPE (%)
BA	FMNP	3.9894	2.8879	1.5135	1.5109
	Naïve	3.9923	2.8882	1.5139	1.5113
OIL	FMNP	1.5601	1.2176	1.4763	1.4737
	Naïve	1.5651	1.2204	1.4798	1.4772
HAL	FMNP	0.7573	0.5649	1.6555	1.6538
	Naïve	0.7608	0.5667	1.6617	1.6598
SLB	FMNP	1.0097	0.7429	1.5269	1.5260
	Naïve	1.0129	0.7456	1.5326	1.5316

5 Discussion

This section discusses the implications of the findings on the basis of the experimental results and the potential limitations of this study. First, utilizing the movement prediction of the exogenous variable as the indirect movement prediction of the target variable proves to be effective and robust. Considering the length of each time series, which covers a period of approximately 10 years, the movement prediction provided by the actual movement of the FTSE open price can be considered to be consistent across the whole period. Nonetheless, although many studies have questioned the effectiveness of neural networks for point forecasting in random walks, this does not necessarily mean that advanced machine learning or deep learning models cannot be used to provide accurate movement prediction. As summarized by Bustos and Pomares-Quimbaya (2020), the movement prediction accuracy of financial time series can reach as high as 0.8 in specific scenarios; therefore, high movement prediction for real-world random walks is possible and can potentially lead to better fusion results than the examples shown in this study.

Second, the fusion process can be seen as a classification-to-regression conversion within the context of symmetric random walk forecasting. While many forecasting scenarios require the integration of diverse predictions to enhance decision-making, effectively combining predictions from models that produce different types of outputs, such as binary and continuous data, remains a challenge (Bishop & Nasrabadi, 2006; C. Zhang et al., 2022). The FMNP method proposed in this study successfully converts binary classifications (movement predictions) into continuous values (point forecasts), enabling the integration of diverse data types and facilitating the comprehensive utilization of available forecasts to improve decision-making in real-world forecasting scenarios.

Third, while binary or categorical variables are commonly used as features in forecasting, this study shows that it is sufficient to consider only movement prediction and naïve prediction as features. The simulation study demonstrates that the performance of FMNP improves as the movement prediction accuracy increases. Instead of prioritizing the development of complex regression models, we could place emphasis on identifying suitable exogenous variables that can reliably contribute to accurate movement predictions for the target variable. In this context, variable selection, rather than feature selection, is essential for achieving accurate point forecasting in random walks via the proposed FMNP method.

6 Conclusion

This study introduces FMNP, a novel forecasting method designed to improve point forecasts in the challenging context of symmetric random walks. The FMNP reformulates the target variable’s future value as a linear combination of its future movement and current value, offering a straightforward yet effective approach to leveraging movement predictions. The simulation results demonstrate that FMNP can achieve statistically significant improvements over naïve predictions, even with movement prediction accuracies only slightly above 50%. Empirical evaluations on the four U.S. financial time series—Boeing, Brent crude oil, Halliburton, and Schlumberger—using the FTSE index as an exogenous variable further validate FMNP’s practical effectiveness. In all the cases, FMNP outperformed the naïve prediction, highlighting its efficacy and potential applicability to a broader range of forecasting tasks. These findings provide evidence that symmetric random walks are partially predictable and highlight the significant potential of using movement predictions to address the inherent challenges of point forecasting in random walks.

There are several avenues for further research that build upon the foundations laid by this study. First, while this research focuses on symmetric random walk forecasting, future work could explore applying the forecasting philosophy presented here to other types of time series, potentially broadening its applicability. Second, this study provides a simple

and robust approach for obtaining movement prediction of the target variable by leveraging the actual movement of an exogenous variable. However, identifying the most suitable exogenous variable and further improving the movement prediction accuracy still require much future work.

Moreover, the proposed method uses a fixed increment for simplicity; however, adapting this increment on the basis of the availability of new data may provide more dynamic and accurate forecasts. Investigating whether such adaptive increments can further refine the forecasting accuracy represents a promising direction for future research.

Acknowledgments

This study did not receive any specific grants from funding agencies in the public, commercial, or not-for-profit sectors.

References

- Adhikari, R., & Agrawal, R. (2014). A combination of artificial neural network and random walk models for financial time series forecasting. *Neural Computing and Applications*, 24, 1441–1449. <https://doi.org/10.1007/s00521-013-1386-y>
- Aliferis, C., & Simon, G. (2024). Overfitting, underfitting and general model overconfidence and under-performance pitfalls and best practices in machine learning and ai. In *Artificial intelligence and machine learning in health care and medical sciences: Best practices and pitfalls* (pp. 477–524). Springer. https://doi.org/10.1007/978-3-031-39355-6_10
- Baumeister, C., Guérin, P., & Kilian, L. (2015). Do high-frequency financial data help forecast oil prices? the midas touch at work. *International Journal of Forecasting*, 31(2), 238–252. <https://doi.org/10.1016/j.ijforecast.2014.06.005>
- Bishop & Nasrabadi. (2006). *Pattern recognition and machine learning*. Springer.
- Bustos, O., & Pomares-Quimbaya, A. (2020). Stock market movement forecast: A systematic review. *Expert Systems with Applications*, 156, 113464. <https://doi.org/10.1016/j.eswa.2020.113464>
- Cheng, C., Sa-Ngasoongsong, A., Beyca, O., Le, T., Yang, H., Kong, Z., & Bukkapatnam, S. T. (2015). Time series forecasting for nonlinear and non-stationary processes: A review and comparative study. *Iie Transactions*, 47(10), 1053–1071. <https://doi.org/10.1080/0740817X.2014.999180>
- Christen, R., Mazzola, L., Denzler, A., & Portmann, E. (2022). Distance metrics for evaluating the use of exogenous data in load forecasting. *International Conference on Information Processing and Management of Uncertainty in Knowledge-Based Systems*, 469–482. https://doi.org/10.1007/978-3-031-08974-9_37
- De Gooijer, J. G., et al. (2017). *Elements of nonlinear time series analysis and forecasting* (Vol. 37). Springer.
- Drummond & Holte. (2005). Severe class imbalance: Why better algorithms aren't the answer. In *Machine learning: Ecml 2005* (pp. 539–546). Springer Berlin Heidelberg.
- Ellwanger & Snudden. (2023). Forecasts of the real price of oil revisited: Do they beat the random walk? *Journal of Banking & Finance*, 154, 106962. <https://doi.org/10.1016/j.jbankfin.2023.106962>
- Engle. (2004). Risk and volatility: Econometric models and financial practice. *American Economic Review*, 94(3), 405–420. <https://doi.org/10.1257/0002828041464597>
- Fama, E. F. (1995). Random walks in stock market prices. *Financial analysts journal*, 51(1), 75–80.
- Gupta, R., Haddad, S., & Selvanathan, E. (2024). Global power and stock market co-movements: A study of g20 markets. *Global Finance Journal*, 62, 101028. <https://doi.org/10.1016/j.gfj.2024.101028>
- Hewamalage, H., Ackermann, K., & Bergmeir, C. (2023). Forecast evaluation for data scientists: Common pitfalls and best practices. *Data Mining and Knowledge Discovery*, 37(2), 788–832. <https://doi.org/10.1007/s10618-022-00894-5>
- Ibe. (2014). *Fundamentals of applied probability and random processes*. Academic Press.
- Jadecivicius, A., & Huston, S. (2015). Property market modelling and forecasting: Simple vs complex models. *Journal of Property Investment & Finance*, 33(4), 337–361. <https://doi.org/10.1108/JPIF-08-2014-0053>
- Jiang. (2021). Applications of deep learning in stock market prediction: Recent progress. *Expert Systems with Applications*, 184. <https://doi.org/10.1016/j.eswa.2021.115537>
- Josephine, S. A. (2017). Predictive accuracy: A misleading performance measure for highly imbalanced data classified negative. *SAS Global Forum*, 1–12.
- Junninen, H., Niska, H., Tuppurainen, K., Ruuskanen, J., & Kolehmainen, M. (2004). Methods for imputation of missing values in air quality data sets. *Atmospheric environment*, 38(18), 2895–2907. <https://doi.org/10.1016/j.atmosenv.2004.02.026>
- Kilian, L., & Taylor, M. P. (2003). Why is it so difficult to beat the random walk forecast of exchange rates? *Journal of International Economics*, 60(1), 85–107. [https://doi.org/10.1016/S0022-1996\(02\)00060-0](https://doi.org/10.1016/S0022-1996(02)00060-0)

- Lara-Benítez, P., Carranza-García, M., & Riquelme, J. C. (2021). An experimental review on deep learning architectures for time series forecasting. *International journal of neural systems*, 31(03), 2130001. <https://doi.org/10.1142/S0129065721300011>
- Li & Johnson. (2014). Wilcoxon's signed-rank statistic: What null hypothesis and why it matters. *Pharmaceutical Statistics*, 13(5), 281–285. <https://doi.org/10.1002/pst.1628>
- Ma, Y., Mao, R., Lin, Q., Wu, P., & Cambria, E. (2023). Multi-source aggregated classification for stock price movement prediction. *Information Fusion*, 91, 515–528. <https://doi.org/10.1016/j.inffus.2022.10.025>
- Montesinos López, O. A., Montesinos López, A., & Crossa, J. (2022). Overfitting, model tuning, and evaluation of prediction performance. In *Multivariate statistical machine learning methods for genomic prediction* (pp. 109–139). Springer. https://doi.org/10.1007/978-3-030-89010-0_4
- Moosa. (2013). Why is it so difficult to outperform the random walk in exchange rate forecasting? *Applied Economics*, 3340–3346. <https://doi.org/10.1080/00036846.2012.709605>
- Moosa & Burns. (2014). The unbeatable random walk in exchange rate forecasting: Reality or myth? *Journal of Macroeconomics*, 40, 69–81. <https://doi.org/10.1016/j.jmacro.2014.03.003>
- Moosa & Burns. (2016). The random walk as a forecasting benchmark: Drift or no drift? *Applied Economics*, 48(43), 4131–4142. <https://doi.org/10.1080/00036846.2016.1153788>
- Pearson. (1905). The problem of the random walk. *Nature*, 72(1865), 294–294. <https://doi.org/10.1038/072294b0>
- Petropoulos, F., Apiletti, D., Assimakopoulos, V., Babai, M. Z., Barrow, D. K., Taieb, S. B., Bergmeir, C., Bessa, R. J., Bijak, J., Boylan, J. E., et al. (2022). Forecasting: Theory and practice. *International Journal of Forecasting*, 38(3), 705–871. <https://doi.org/10.1016/j.ijforecast.2021.11.001>
- Rogers, A. (1995). Population forecasting: Do simple models outperform complex models? *Mathematical Population Studies*, 5(3), 187–202. <https://doi.org/10.1080/08898489509525401>
- Sarwar. (2020). Interrelations in market fears of U.S. and European equity markets. *The North American Journal of Economics and Finance*, 52, 101136. <https://doi.org/10.1016/j.najef.2019.101136>
- Scabbia, G., Sanfilippo, A., Bachour, D., & Perez-Astudillo, D. (2020). Exogenous parameters in solar forecasting. *2020 47th IEEE Photovoltaic Specialists Conference (PVSC)*, 0894–0896.
- Sezer, O. B., Gudelek, M. U., & Ozbayoglu, A. M. (2020). Financial time series forecasting with deep learning: A systematic literature review: 2005–2019. *Applied soft computing*, 90, 106181. <https://doi.org/10.1016/j.asoc.2020.106181>
- Taylor. (2008). *Modelling financial time series*. World Scientific.
- Thakkar & Chaudhari. (2021). Fusion in stock market prediction: A decade survey on the necessity, recent developments, and potential future directions. *Information Fusion*, 65, 95–107. <https://doi.org/10.1016/j.inffus.2020.08.019>
- Tsantekidis, A., Passalis, N., Tefas, A., Kannianen, J., Gabbouj, M., & Iosifidis, A. (2020). Using deep learning for price prediction by exploiting stationary limit order book features. *Applied Soft Computing*, 93, 106401. <https://doi.org/10.1016/j.asoc.2020.106401>
- Weng, B., Ahmed, M. A., & Megahed, F. M. (2017). Stock market one-day ahead movement prediction using disparate data sources. *Expert Systems with Applications*, 79, 153–163. <https://doi.org/10.1016/j.eswa.2017.02.041>
- Wergen, G., Majumdar, S. N., & Schehr, G. (2012). Record statistics for multiple random walks. *Physical Review E—Statistical, Nonlinear, and Soft Matter Physics*, 86(1), 011119. <https://doi.org/10.1103/PhysRevE.86.011119>
- Wu, C., Wang, J., & Hao, Y. (2022). Deterministic and uncertainty crude oil price forecasting based on outlier detection and modified multi-objective optimization algorithm. *Resources Policy*, 77, 102780. <https://doi.org/10.1016/j.resourpol.2022.102780>
- Wu, H., Xu, J., Wang, J., & Long, M. (2021). Autoformer: Decomposition transformers with auto-correlation for long-term series forecasting. *Advances in neural information processing systems*, 34, 22419–22430.
- Zeng, A., Chen, M., Zhang, L., & Xu, Q. (2023). Are transformers effective for time series forecasting? *Proceedings of the AAAI conference on artificial intelligence*, 37(9), 11121–11128. <https://doi.org/10.1609/aaai.v37i9.26317>
- Zhang, C., Sjarif, N. N., & Ibrahim, R. B. (2022). Decision fusion for stock market prediction: A systematic review. *IEEE Access*, 10, 81364–81379. <https://doi.org/10.1109/ACCESS.2022.3195942>
- Zhang, C., Sjarif, N. N. A., & Ibrahim, R. (2024). Deep learning models for price forecasting of financial time series: A review of recent advancements: 2020–2022. *Wiley Interdisciplinary Reviews: Data Mining and Knowledge Discovery*, 14(1), e1519. <https://doi.org/10.1002/widm.1519>
- Zhang, J.-L., Zhang, Y.-J., & Zhang, L. (2015). A novel hybrid method for crude oil price forecasting. *Energy Economics*, 49, 649–659. <https://doi.org/10.1016/j.eneco.2015.02.018>
- Zhang, Y.-C. (1999). Toward a theory of marginally efficient markets. *Physica A: Statistical Mechanics and its Applications*, 269(1), 30–44. [https://doi.org/10.1016/S0378-4371\(99\)00077-1](https://doi.org/10.1016/S0378-4371(99)00077-1)
- Zhou, T., Ma, Z., Wen, Q., Wang, X., Sun, L., & Jin, R. (2022). Fedformer: Frequency enhanced decomposed transformer for long-term series forecasting. *International conference on machine learning*, 27268–27286.